PACE-2021
International Congress on the Phenomenological Aspects of Civil Engineering
Research Article 20-23 June 2021

Investigating Soil-Structure Interaction Effects on The Seismic Performance of Setback Buildings

Farshad Homaei
Department of Earthquake and Geotechnical Engineering, Faculty of Civil and Surveying Engineering, Graduate University of Advanced Technology, Kerman, Iran
Corresponding Author E-mail: f.homaei@kgut.ac.ir *Corresponding Author ORCID: 0000-0001-5163-9240*

Keywords

Performance-Based Seismic Response,
Setback Buildings,
Steel Structures,
Soil-Structure Interaction,
Seismic Demand,
Vulnerability.
.

Abstract

Accurate seismic response estimation of structures requires adequate consideration of soil nonlinear behavior and its interaction with the superstructure. This paper presents a comprehensive study on the effect of Soil-Structure Interaction (SSI) on performance-based seismic response of typical mid-rise steel setback buildings and the demand distribution over the structure height. Therefore, foundation flexibility effects are investigated on the maximum displacement, inter-story drift ratio, shear and moment distribution over the structure height, and the maximum plastic hinge rotation of beam and column elements at different story levels. Results show that foundation flexibility alters the demand distribution pattern over the structure height. The level of nonlinear behavior of setback buildings plays a critical role in the structural seismic response. The shear and moment forces reduce due to the SSI effect. Meanwhile, the drift and displacement demand of flexible base setback buildings increases in comparison with the fixed base models. A large portion of demand is concentrated near the base and around the setback area, in a way that the plastic hinges of beam and column elements are affected. Moreover, SSI increases the plastic hinge rotation in beam and column elements. In conclusion, the design of setback building, especially on soft soils requires particular attention.

1.Introduction

Setback buildings are observed to have high damage potential under seismic loads. Unfortunately, evidence represent inadequacy in the seismic behavior of setback buildings during strong ground motions. Site surveying of setback buildings shows a significant increase in the number of damaged buildings. Codebase-designed setback structures are also observed to get seriously damaged during earthquake ground motions [1]. The behavior of these buildings is affected by the combination of mass, stiffness, and strength irregularity over the structure height. Irregularity changes the usual seismic response of the structures and increases the demand and damage potential in buildings.

Generally, the development of plastic hinges at the end of frame elements increases the vulnerability of the structures to seismic loads. The applied force affects the level of demand and increases the rotation of the plastic hinges. Increasing the rotation of frame plastic hinges makes an increase in the displacement and drift demands of the structure. Thus, studying the demand distribution and concentration of damage helps clarify the vulnerability mechanism in structures.

Studies were performed to understand the complex behavior of setback buildings. It was observed that the inter-story drift ratio of setback floors is larger than that of the regular frame at the same story level [2]. Studying the damaged elements has shown that the vulnerability is mostly concentrated at the load resisting components near the setback area [1, 3, 4]. Additionally, the inelastic response of asymmetric floors about the vertical axis of the structure causes the poor seismic performance of the setback buildings [5]. Moreover, the setback ratio values play a critical role in the structural performance of setback buildings [6].

Interaction of the structures with the soil is another issue that makes the seismic response of setback buildings more complex. Generally, the natural vibration period of the flexible-base system increases due to the higher flexibility of the soil. Moreover, foundation flexibility modifies the displacement demand. During earthquake ground motions, the foundation experiences transition, rocking, and torsional movements. This results in settlement, sliding, and rocking movements of the structural system. Meanwhile, this may cause gaps between the soil and the foundation which directly affects the seismic response of the superstructure [7, 8]. Moreover, the nonlinear behavior and hysteretic energy dissipation of the soil can reduce the force demands in the superstructure. Studies were performed to demonstrate the effect of soil nonlinear behavior on the seismic performance of structures[9-18]. Some of these studies aimed to show the effect of Soil-Structure Interaction (SSI) on the vulnerability of superstructures [11, 12]. Results have shown that SSI modifies the structural performance [19, 20], varies the demand distribution, and alters the plastic hinge rotation in force-resisting elements [21]. Moreover, increases in the damage index of short periods or slender buildings on soft soil are expected [22]. Therefore, it is encouraged to consider accurate nonlinear material behavior and energy dissipation capability of the soil-foundation system in performance-based earthquake engineering and vulnerability assessment studies [23, 24].

In this study, the effect of SSI is evaluated on the distribution of demand and vulnerability of setback buildings. Time history response of steel structures with several setback ratios is carried out and the performance-based displacement and drift demands of flexible-base setback buildings are compared to those of the fixed-base ones. The maximum shear and moment forces at each story level are calculated to show the SSI effect on force demand distribution. Finally, the maximum plastic hinge rotation of beam and column elements is presented to show the SSI effect on the vulnerability level of structural elements and collapse mechanism in setback buildings at various performance objectives.

2. Soil-Structure Systems

2.1. Typical building configuration

The reference building was considered to be a three-dimensional mid-rise steel building with regular configuration. As shown in Figure 1, five uniformly spaced frames with a bay length of 5m were connected at two orthogonal directions to build the configuration of the reference regular structure. Although the bay width of 4 to 6m is quite low in American practice, it is common in European and Middle East practice [6]. This building has ten levels and a floor-to-floor height of 3m. The structure occupancy was considered to be residential. Therefore, based on the recent edition of the Iranian building national code [25], gravity loads of 6.9kPa and 1.96kPa were assigned to each story floor as dead and live loads, respectively. It is worth mentioning that the floors consisted of rigid diaphragms.

The occupancy and framing configuration of setback buildings were considered to be similar to those of the reference regular structure. However, setback buildings were formed by one-sided elimination of top floors' effective area. This divides a setback building into two parts. The lower part with the largest floor area is usually termed "the base" and the upper part with the smallest floor area is termed "the tower". In the present study, the categorization of setback buildings was performed by using two indexes:

$$R_A = \frac{Area\ of\ Tower}{Area\ of\ Base} \quad (1)$$

$$R_H = \frac{Height\ of\ Tower}{Height\ of\ Base} \quad (2)$$

where R_A shows the ratio of story area at "the tower" to "the base". The frame bays of the reference structure were removed along the structural axis to make setback buildings. Thus, the elimination of three, two and one bays give three categories for R_A: R_A=0.25, R_A=0.50, and R_A=0.75 Similarly, RH represents the relative height of "the tower" to "the base" [3, 6]. Three categories were selected for R_H as well: R_H=3/7 R_H=5/5 and R_H=7/3. These values show the locality of the setback floor at the 7th, 5th, and 3rd levels, respectively. Figure 2 shows the geometry of the studied setback buildings. It is worth mentioning that there were deficiencies in the classification of irregular buildings in the previous edition of the Iranian seismic design code [29]. Additionally, the SSI effect is not considered in the design procedure. However, this was rectified in the current edition [26] to modify the analysis results and consider the SSI effect in the design procedure.

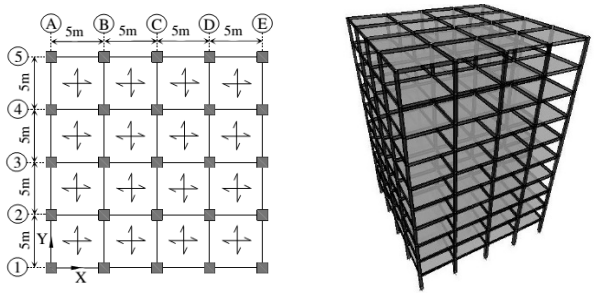

Figure 1. Plan, and three-dimensional view of the reference regular structure

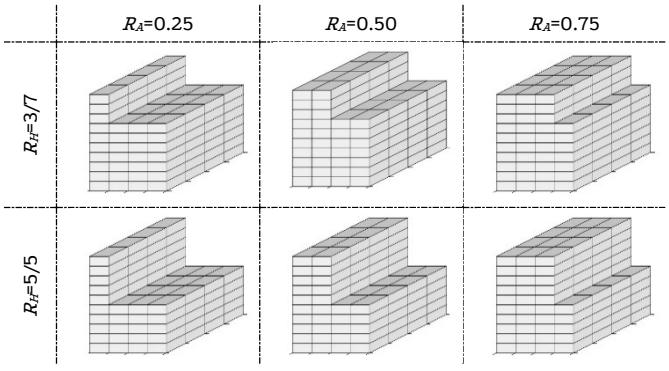

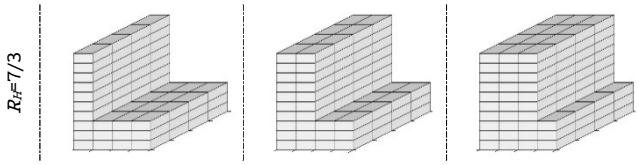

Figure 2. Setback structure

2.2. Seismic design of structures

The seismic design of the structures was accomplished according to the recent edition of the Iranian seismic design code [26]. The structures were assumed on a hypothetical site in metropolitan Tehran, Iran. According to this code [26], the seismic hazard zone of Tehran is categorized as "very high" with a site-specific acceleration of 0.35g. The code-base-designed structures are expected to satisfy the life safety performance level under the seismic hazard level with a 10% probability of exceedance in 50 years [26].

According to the Iranian steel design code [30], the structural frame elements were designed based on the Load and Resistance Factor Design (LRFD) method. The design procedure of this code is similar to that of ANSI/AISC 360-10 [31]. The lateral force-resisting system of steel frames was considered as a special (ductile) moment resisting system with fully restrained moment connections (cover-plated flange type). Finally, IPE270 to IPE550 were selected for the beam sections and the square tube sections were assigned to the column elements. The dimension of column sections varies from 200×200×15mm to 460×460×25mm. Table 2 shows the material properties of the beam and column sections.

Table 1. Steel material properties

Yield stress	$F_y = 240\,MPa$
Modulus of elasticity	$E = 200\ GPa$
Poisson ratio	$\upsilon = 0.3$

2.3. The soil and foundation system

Iranian seismic design code [26] classifies the soil types into four categories. The soil in the north of Tehran is classified as type I with the shear wave velocity of V_{s30}>750m/s at the depth of 30m from the ground surface [32]. Meanwhile, the soil in the south of Tehran has a shear wave velocity of 175m/s< V_{s30}<375m/s and is categorized as type III [33].

As the effect of SSI is more predominant for structures on soft soil [34], the soil under the foundation was assumed as type III with the shear wave velocity V_{s30}=200m/s. The material properties of the soil were listed in

Table 3. The design of the foundation system was accomplished based on the allowable stresses of soil. According to the Iranian foundation design code [35], the safety factors of 3.0 and 1.5 were applied to the bearing and sliding capacity of the strip foundations. Finally, appropriate dimensions were selected for strip foundations as shown in Table 4. Figure 3 shows the outline of strip footings at the base level of structures. As it is observed, each strip foundation was connected to the adjacent one across the column axis. This makes the coordinated movement of foundations during earthquake ground motions. The connectors were designed to withstand a tension force equal to 10% of the maximum columns axial load.

Table 2. Soil material properties

Parameter	Symbol	Value
Mass density	ρ	1900 Kg/m^3
Elastic Modulus	E	2.025×10^8 N/m^2
Shear modulus	G	7.5×10^7 N/m^2
Poisson's ratio	υ	0.35
Friction Angle	φ	35°
Cohesion	c	0 N/m^2

Table 3. Foundation dimensions (L: length, B: width, H: thickness).

Structural Model		Foundation dimensions Middle $L\times B\times H\ (cm)$	Foundation dimensions Side $L\times B\times H\ (cm)$
Regular		2200×110×60	2200×60×60
$R_H=3/7$	$R_A=0.25$	2200×90×60	2200×50×60
	$R_A=0.50$	2200×105×60	2200×55×60
	$R_A=0.75$	2200×110×60	2200×55×60
$R_H=5/5$	$R_A=0.25$	2200×80×50	2200×40×50
	$R_A=0.50$	2200×95×50	2200×45×50
	$R_A=0.75$	2200×100×50	2200×50×50
$R_H=7/3$	$R_A=0.25$	2200×65×40	2200×40×40
	$R_A=0.50$	2200×80×40	2200×40×40
	$R_A=0.75$	2200×95×40	2200×50×40

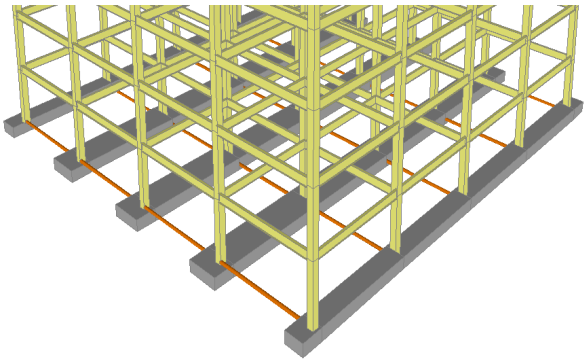

Figure 3. The foundation system

3. Nonlinear modeling

The three-dimensional nonlinear modeling of the soil-structure system was accomplished in "Open System for Earthquake Engineering Simulation (OpenSees)" [36]. The damping ratio of the system was considered 5%. The Rayleigh damping method was used to model the viscous damping [37]. The P-Delta effect was considered in the geometric transformation of the frame elements. The nonlinear models of frame elements and soil-foundation systems were prepared by using the material library of OpenSees. Detailed discussions are presented in the subsequent sections.

3.1. Frame elements

The nonlinear material behavior of beam and column elements was modeled by using lumped plastic hinges at the end of frame elements. The plastic hinges follow the modified Ibarra-Medina-Krawinkler deterioration model with a bilinear hysteretic response. The backbone curve of this material is shown in Figure 4. Provisions in ASCE41-13 [38] were used to determine the parameter specification of this material. Furthermore, moderate cyclic deterioration in loading and unloading stiffness of the hinge elements was considered [39]. The relations developed by Lignos and Krawinkler [40, 41] were used for the hysteretic response of this material.

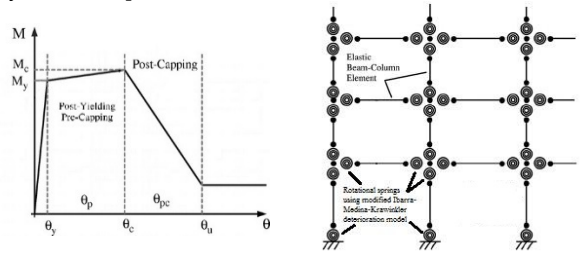

* M_y : The yielding moment capacity of the section

* M_c : The capping moment capacity of the section

* θ_y : The rotation of the hinge at the yielding point

* θ_c : The rotation of the hinge at the capping points

Figure 4. Component of the backbone curve of frame elements hinge

3.2. Soil and foundation elements

The theory of Beam on the Nonlinear Winkler Foundation (BNWF) was used to model the soil-foundation system. This method is observed to be capable of capturing the experimentally observed behavior of shallow foundations [21, 42-47]. The footing members are modeled with elastic beam elements and a series of vertical and horizontal springs are used to model the soil behavior. Figure 5 shows the component of BNWF. Three sets of springs are used to model the foundation flexibility effect.

The vertical springs are known as q-z and are used to capture the vertical and rotational resistance of the footing against the applied loads. Furthermore, the yielding of soil material in compression and separation of the footing from the soil surface in tension is modeled by these elements.

The passive resistance of soil, as well as the sliding of footing on the soil surface, is captured by two sets of horizontal springs. The p-y spring simulates the passive resistance of the footing. The t-z spring is used to model the cohesion and friction resistance of the footing on the soil surface. This element is capable of simulating the slippage of the footing on the soil surface.

Figure 6 shows the nonlinear backbone curve of q-z, t-z, and p-y springs. The asymmetric hysteretic response of q-z springs is expressed with the ultimate load capacity of soil on the compression side and reduced strength in tension. The t-z spring has a backbone curve with broad hysteresis behavior. The pinched hysteretic behavior of p-y spring is used to model the gapping phenomenon during unloading on one side of the foundation.

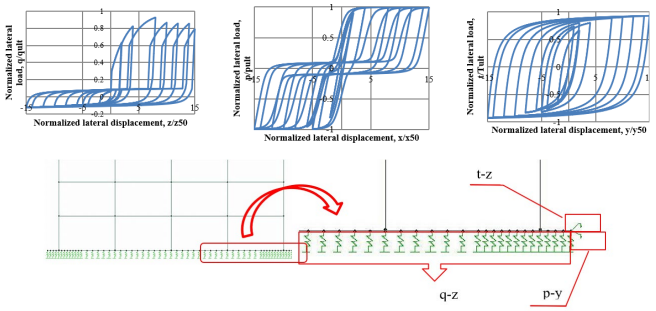

Figure 5. Beam on nonlinear Winkler foundation model

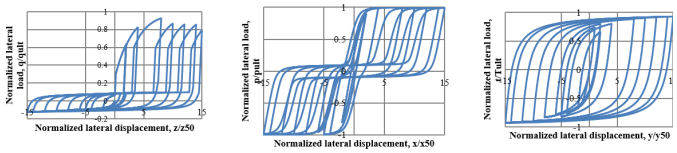

Figure 6. Nonlinear backbone curve of soil springs: a) q-z, b) p-y, c) t-z

Boulanger et al. [48] and Boulanger [49] described the equations of the backbone curve of BNWF springs. The applied load (F) and the corresponding displacement (δ) are assumed linearly proportional at the primary steps of the applied load:

$$F = k_{in}\delta \tag{3}$$

Where k_{in} is the initial elastic stiffness of each soil spring. ASCE41-13 [38], proposes equations for determining the initial stiffness of soil. The yielding capacity of the soil material (F_0) is assumed proportionally dependent on the ultimate bearing capacity (F_{ult}):

$$F_0 = C_r F_{ult} \tag{4}$$

where Cr is the parameter that controls the range of elastic behavior. The post-yielding nonlinear behavior of soil is defined as:

$$F = F_{ult} - (F_{ult} - F_0)\left[\frac{c\delta_{50}}{c\delta_{50} + |\delta^p - \delta_0^p|}\right]^n \quad (5)$$

In this equation, δ50 represents the displacement corresponding to 50% of the ultimate load, δ_0^p is the displacement at the yielding point, δ^p is the displacement in the post-yield region and c and n are parameters that control the post-yield shape of the backbone curve. These two parameters were calibrated for sandy or clay soils in common finite element software like OpenSees [49, 50]. Thus, the two main parameters that control the shape of the backbone curve are F_{ult} and δ_{50}.

The developed equations like Terzaghi [51] give the ultimate capacity of the soil (Fult). Harden et al. [47] proposed relations for δ_{50} as:

$$\text{q-z spring } (\delta_{50} \to z_{50}; F_{ult} \to q_{ult}): \begin{cases} z_{50} = 1.390\dfrac{q_{ult}}{k_{in}} & \text{for sand} \\ z_{50} = 0.525\dfrac{q_{ult}}{k_{in}} & \text{for clay} \end{cases}$$

$$\text{p-y spring } (\delta_{50} \to x_{50}; F_{ult} \to p_{ult}): \begin{cases} x_{50} = 0.542\dfrac{p_{ult}}{k_{in}} & \text{for sand} \\ x_{50} = 8.0\dfrac{p_{ult}}{k_{in}} & \text{for clay} \end{cases} \quad (6)$$

$$\text{t-z spring } (\delta_{50} \to y_{50}; F_{ult} \to t_{ult}): \quad y_{50} = 2.050\frac{t_{ult}}{k_{in}}$$

The material behavior of q-z t-z and p-y springs was developed in OpenSees and used to model the soil flexibility effects. The distribution of the soil springs along the foundation base was performed based on the recommendation by Harden et al. [47]. The experimental tests showed the necessity to use tighter spring spacing at the end region of the foundation to increase the end length stiffness (Figure 5). Thus, the vertical springs were spaced at a distance of 12.5cm at the end regions and spread out up to 25 cm elsewhere.

It has to be pointed out that the torsional response of irregular buildings makes the foundation rotate about the vertical axis of the structure. Therefore, a rotational spring was used to consider the torsional response of the foundation on the soil surface in three-dimensional models. The properties of this spring were adopted based on ASCE 41-13 [38].

4. Analysis procedure and performance criteria

4.1. Incremental dynamic analysis

The seismic response of fixed and flexible-based structures was evaluated from the elastic phase of behavior to their highly nonlinear and up to the collapse point, by using Incremental Dynamic Analysis (IDA). In this procedure, the earthquake records are incrementally scaled from the initial spectral intensity equal to 0.01g and increase monotonically with an incremental spectral intensity equal to 0.05g. The results from the gradual increase of the ground motions intensity are utilized for generating the IDA curves and assessing the structural performance levels. A sample of these curves was developed and plotted in Figure 7.

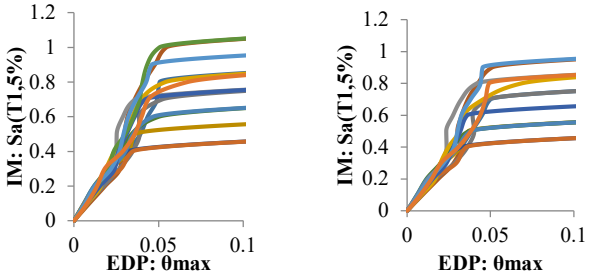

a) Fixed-base b) Flexible-base

Figure 7. The IDA curves of regular structure: a) fixe base b) flexible base conditions

4.2. Site characterization and seismic hazard

The studied buildings are located in a hypothetical site (51.36E, 35.67N) in metropolitan Tehran, Iran. This city is surrounded by such faults as "Mosha fault", "North Tehran fault", "Kahrizak fault" and "Eyvanekey fault" (Figure 8). The site-specific spectra were considered according to the uniform hazard spectrum (UHS) method for scaling records in order to predict adequate structural response. In this procedure, the uniform hazard spectrum for soil site class III was used from the Iranian seismic design code [26].

4.3. Ground motion selection

The selection of ground motions was performed from the PEER-NGA database [52]. The selection procedure was carried out based on the spectrum matching of the ground motions to that of the uniform hazard spectrum in the Iranian Seismic design code [26]. In this procedure, the Square Root of the Sum of the Squares (SRSS) of the response spectrum of horizontal components of the ground motions is calculated. Then, the ground motions were scaled so that their SRSS response spectrum closely matched to the target spectrum over the period range of 0.2T to1.5T; where T is the first-mode vibration period of the structure [53]. The first-mode vibration period of the fixed and flexible-base regular and setback buildings was shown in Table 5. Results show that foundation flexibility increases the vibration period of the structures up to 2.5%.

In the next step, the final ensemble of the ground motions was adjusted based on appropriate values of average shear-wave velocity, magnitude, and closest distance to the fault rupture. The average shear-wave velocity at the top 30m of the soil was considered to be 175m/s to 375m/s and close to 200m/s. The magnitude (M) of the earthquakes was chosen to be relatively large (6-7.6) and the closest distance to fault rupture (R) was considered moderately between 20 to 50km with no marks of directivity.

The final ensemble of 20 ground motions was shown in Table 6. Figure 9 shows the mean linear response spectrum of the ensemble ground motions in comparison to the target spectrum. It is observed that the mean spectrum matches reasonably well with the target spectrum for the period range related to the regular structure. The same spectrum matching was checked in the setback buildings.

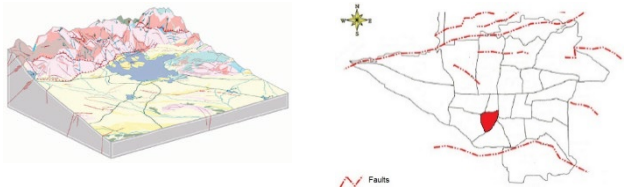

Figure 8. The considered site and the known earthquake faults in metropolitan Tehran, Iran

Table 4. Fundamental periods of studied buildings

Structural Model		Fixed-base (sec)	Flexible-base (sec)
Regular		2.05	2.10
	$R_A = 0.25$	1.88	1.91
$R_H = 3/7$	$R_A = 0.50$	1.95	1.98
	$R_A = 0.75$	2.03	2.06
	$R_A = 0.25$	1.69	1.72
$R_H = 5/5$	$R_A = 0.50$	1.87	1.90
	$R_A = 0.75$	2.00	2.03
	$R_A = 0.25$	1.70	1.73
$R_H = 7/3$	$R_A = 0.50$	1.92	1.96
	$R_A = 0.75$	2.03	2.05

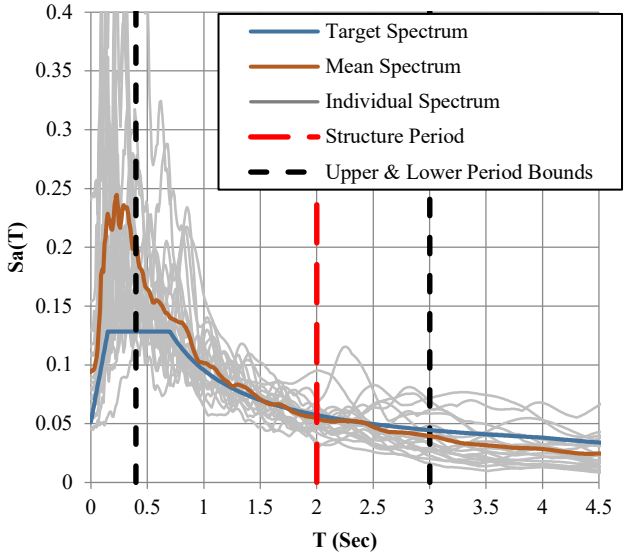

Figure 9. Comparison between the target spectrum and the mean spectrum of the ensemble ground motions

4.4. Selection of critical component of ground motions

Due to the irregular configuration of setback buildings, it is important to apply the components of the earthquake ground motions in an appropriate direction to see the most critical structural response. The selection of the critical component of ground motions was performed base on the maximum Specific Energy Density (*SED*) [54, 55] among the two horizontal components of each earthquake record. The SED of an earthquake record is expressed as:

$$SED = \int_0^t \left[V(t)\right]^2 dt \tag{7}$$

Where V(t) is the velocity-time history of the ground motion. The SED of the selected ground motions was calculated and shown in Table 7.
To perform dynamic analysis with the simultaneous action of two orthogonal ground motions, the scaling factor of both components was considered to be identical. This maintains the relative properties of strong and weak components in the analysis. It is worth mentioning that the level of seismic intensity (IM) corresponds to the strong component.
The critical direction for the application of the earthquake records was specified by a series of nonlinear analyzes. The critical response of the structure was observed as the strong component was applied parallel to the X-axis (Figure 2). Note that this is in agreement with the experimental results by Shahrooz et al. [4].

Table 5. The ensemble of 20 earthquake ground motions

No.	Earthquake Name	Year	Station Name	Magnitude
1	Northridge-01	1994	Lawndale - Osage Ave	6.69
2	Northridge-01	1994	Playa Del Rey - Saran	6.69
3	Kobe_ Japan	1995	Yae	6.9
4	Chi-Chi_ Taiwan	1999	CHY033	7.62
5	Chi-Chi_ Taiwan	1999	CHY082	7.62
6	Chi-Chi_ Taiwan	1999	TCU098	7.62
7	Chi-Chi_ Taiwan	1999	WTC	7.62
8	Manjil_ Iran	1990	Qazvin	7.37
9	Imperial Valley-06	1979	Calipatria Fire Station	6.53
10	Imperial Valley-06	1979	El Centro Array #13	6.53
11	Loma Prieta	1989	Salinas - John & Work	6.93
12	Chi-Chi_ Taiwan-06	1999	TCU051	6.3
13	Chi-Chi_ Taiwan-06	1999	TCU108	6.3
14	Landers	1992	North Palm Springs Fire Sta #36	7.28
15	Landers	1992	Thousand Palms Post Office	7.28
16	San Simeon_ CA	2003	San Luis Obispo - Lopez Lake Grounds	6.52
17	Morgan Hill	1984	Fremont - Mission San Jose	6.19
18	Morgan Hill	1984	San Juan Bautista_ 24 Polk St	6.19
19	Landers	1992	Mission Creek Fault	7.28
20	Tabas	1978	Ferdows	7.35

Table 6. Properties of the component of ground motions

No.	Week Component			Strong Component		
	PGA (g)	PGV (cm/s)	SED (cm2/s)	PGA (g)	PGV (cm/s)	SED (cm2/s)
1	0.081	10.15	240.59	0.147	9.05	251.82
2	0.143	15.33	509.09	0.070	15.23	805.36
3	0.147	21.74	2103.83	0.158	21.19	3273.66
4	0.060	17.13	2225.78	0.069	19.43	2264.77
5	0.062	18.58	2820.08	0.064	20.96	3823.01
6	0.100	27.30	2716.60	0.105	45.66	8086.12
7	0.050	9.59	384.49	0.054	17.82	1987.79
8	0.131	10.95	431.16	0.184	15.49	449.35
9	0.079	13.66	494.26	0.129	15.60	785.27
10	0.139	13.64	597.67	0.116	16.08	616.08
11	0.058	6.26	123.23	0.109	11.22	211.71
12	0.051	5.90	52.05	0.048	5.57	70.81
13	0.065	6.24	172.77	0.070	7.46	176.94
14	0.139	11.54	537.44	0.139	14.62	1337.80
15	0.116	13.83	1054.10	0.100	20.21	1267.76
16	0.118	12.46	372.87	0.133	13.10	512.75
17	0.026	2.74	25.09	0.021	3.42	39.57
18	0.044	4.37	59.80	0.036	4.69	62.92
19	0.126	6.79	215.82	0.132	14.61	976.11
20	0.093	5.42	59.71	0.105	7.13	137.54

5. Performance-based structural limit state capacities

Regular and setback buildings with fixed and flexible base conditions were excited under the horizontal action of orthogonal components of ground motions by using the IDA approach. The performance-based seismic capacity of the structures was assessed from the IDA curves. Four common performance levels, namely Intermediate Occupancy (*IO*), Life Safety (*LS*), Collapse prevention (*CP*), and Global Instability (*GI*) were used in the assessment procedure. The IO limit state is defined at the point where θmax=2% [56]. The CP performance level is defined where the tangent slope of the IDA curve reaches 20% of the elastic slope but not far from θmax=10% [56]. The point where θmax is equal to 75% of the CP limit state, represents the LS performance level [57]. The GI performance level is defined as the flat line reaches on the IDA curve [58].
Figure 10 shows the IDA curve of the regular building for fixed and flexible based conditions. Similar curves were developed for other setback buildings, as well. Figure 11 shows the summary results of the performance-based IM capacity of the fixed and flexible-based regular and setback buildings. It is observed that the IM capacity of fixed base structures is higher than that of flexible base buildings. In other words, due to the SSI effect, the performance-based IM capacity of structures decreases in comparison to that of the fixed base ones. Based on these results, the effect of SSI is investigated on the force and displacement demand and damage distribution over the structural height at each limit state.

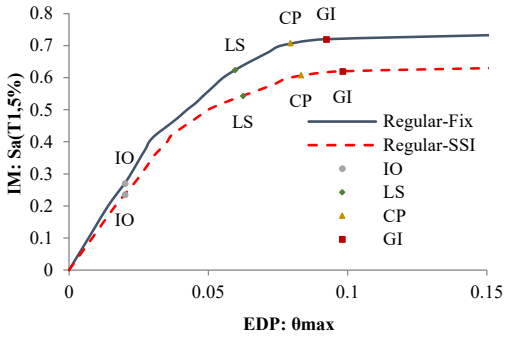

Figure 10. The median IDA curve of regular structure with performance points

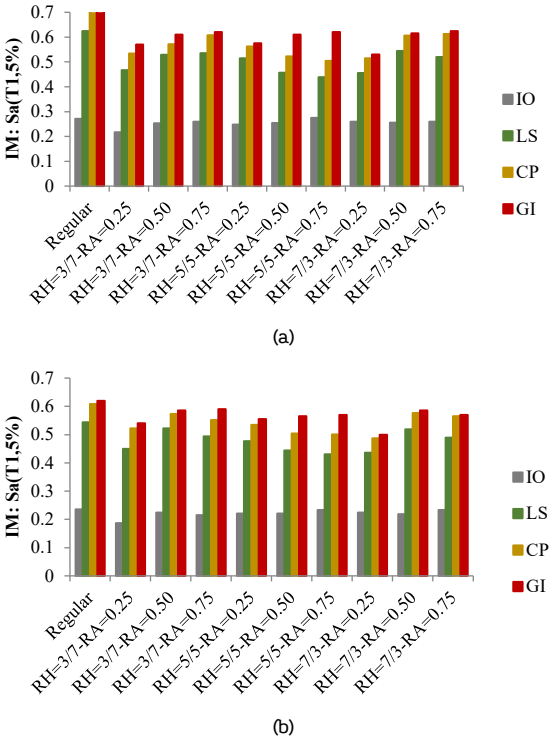

Figure 11. The performance-based IM: (a) fixed-base structures (b) flexible-base structures

6. Results and discussions

6.1. Displacement demand

An interesting question in studying the SSI effect on the seismic response of structures is the displacement demand distribution over the structure height. The maximum displacement of a structure mostly controls the gap space between the two adjacent buildings. In this section, the SSI effect is investigated on the height-wise displacement response of setback buildings at each performance objective. Figure 12 shows the distribution of displacement response over the height of fixed and flexible-base setback buildings and at different performance levels. The filled line refers to the fixed-base buildings and the dashed one represents the displacement response of the flexible-base ones.

Results show that the deformation pattern in flexible-base buildings is similar to that of the fixed-base ones. However, the displacement demand of the flexible-base buildings is greater than the fixed-base ones in most stories. Although this is in agreement with the fact that SSI increases the displacement demand in structures, the rate of increase in the displacement demand is about 8% at the IO limit state. This is more predominant in the case of setback buildings with RH=5/5-RA=0.50, RH=7/3-RA=0.50, and RH=7/3-RA=0.75. A higher rate of increase in the displacement response is observed at the LS and CP performance levels. About a 45% increase happens in the case of structures with RH=3/7-RA=0.25 and RH=5/5-RA=0.50 at the LS limit state. A similar increase is observed in the case of setback buildings with RH=7/3-RA=0.75 and RH=5/5-RA=0.50 at the CP performance level. However, as the structures reach the higher nonlinear phase of behavior (i.e. GI performance level), the variation rate of displacement demand decreases in flexible base buildings so that the maximum difference between the fixed and flexible base structures is about 25% in the case of RH=7/3-RA=0.50.

A comparison between the displacement demand of regular and setback buildings was illustrated in Figure 13. Generally, the flexible base setback buildings give higher values for displacement response in the case of buildings with high ratios of RH and RA. However, the maximum displacement of setback buildings is mostly smaller than that of the regular structure. The maximum difference between the story displacement in regular and setback buildings is observed in the case of RH=7/3-RA=0.25 especially at the nonlinear phase of structural behavior. It is worth mentioning that the effective story mass of setback buildings is smaller than that of the regular building. Hence, the effective earthquake lateral force is lower in these buildings. This causes smaller lateral displacement at different story levels of setback buildings in comparison to that of the regular building. Moreover, the foundation flexibility of the structures moderates the difference between the regular and setback buildings.

6.2. Drift demand

The drift demand shows the level of damage at a story level. The inter-story drift demand for setback buildings at each performance objective was plotted in Figure 14. A comparison between the drift response of fixed and flexible-base buildings shows that SSI increases the maximum drift demand of flexible-base structures. Higher values of demand are observed at the nonlinear phase of behavior. The height-wise drift pattern shows that SSI varies the drift distribution over the structure height. However, the ratio of RH and RA influences the drift response of setback buildings. At the IO performance level, the maximum difference between the drift demand of fixed and flexible-based setback buildings is about 15% and is observed in the case of the structure with RH=7/3-RA=0.25. Meanwhile, the structures with RH=3/7-RA=0.25 and RH=5/5-RA=0.50 show a 47% increase in the drift response at the LS limit state. The difference between the fixed and flexible-based setback buildings reduces as they get to the CP performance level. In this case, about 40% difference is observed for the buildings with RH=5/5-RA=0.50 and RH=7/3-RA=0.75. A similar trend is observed at the GI performance level to increase the demand by up 40% in the case of the structure with RH=3/7-RA=0.25.

Generally, the drift demand is mostly concentrated at the bottom floor of most setback buildings. Meanwhile, depending on the position of the setback floor, a considerable portion of demand is observed near the setback area. It is worth mentioning that SSI also affects the distribution of drift over the structure height. Due to the foundation flexibility effect, the drift demand of setback buildings gives the higher value at the top floors rather than the bottom ones, at the elastic and earlier inelastic phase of the structure behavior. However, at the high nonlinear phase of structural behavior, the drift demand of the bottom floors gives higher values in flexible base setback buildings.

Figure 15 shows the drift demand distribution of the setback buildings at different performance levels in comparison to that of the regular structure. It is observed that the maximum inter-story drift ratio of setback buildings reduces relative to the regular structure. Unlike the regular structure, a large portion of demand is concentrated at the top floors of setback buildings. The rate of demand increases as the performance level of setback building passes from the IO to the GI limit-state. This rate is higher in the case of flexible-base setback buildings so that the difference between the inter-story drift ratio of regular and setback buildings reaches 130%.
The SSI has a moderate effect on the regular structure in comparison to the setback building. It is observed that the maximum difference between the fixed and flexible base regular buildings is up to 11% and it is observed at the high nonlinear phase of structural behavior.

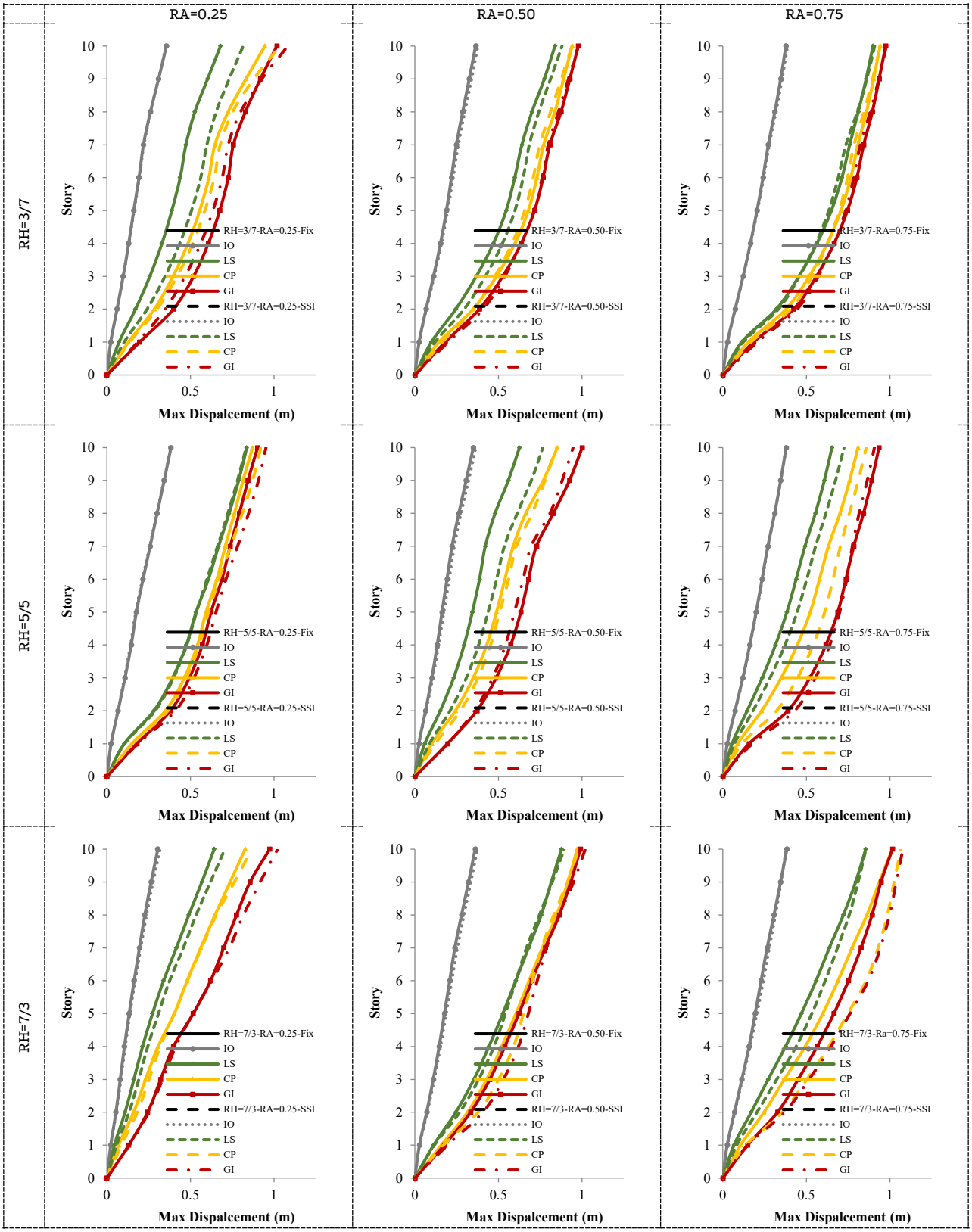

Figure 12. The distribution of displacement demand over the height of fixed and flexible-base setback structures

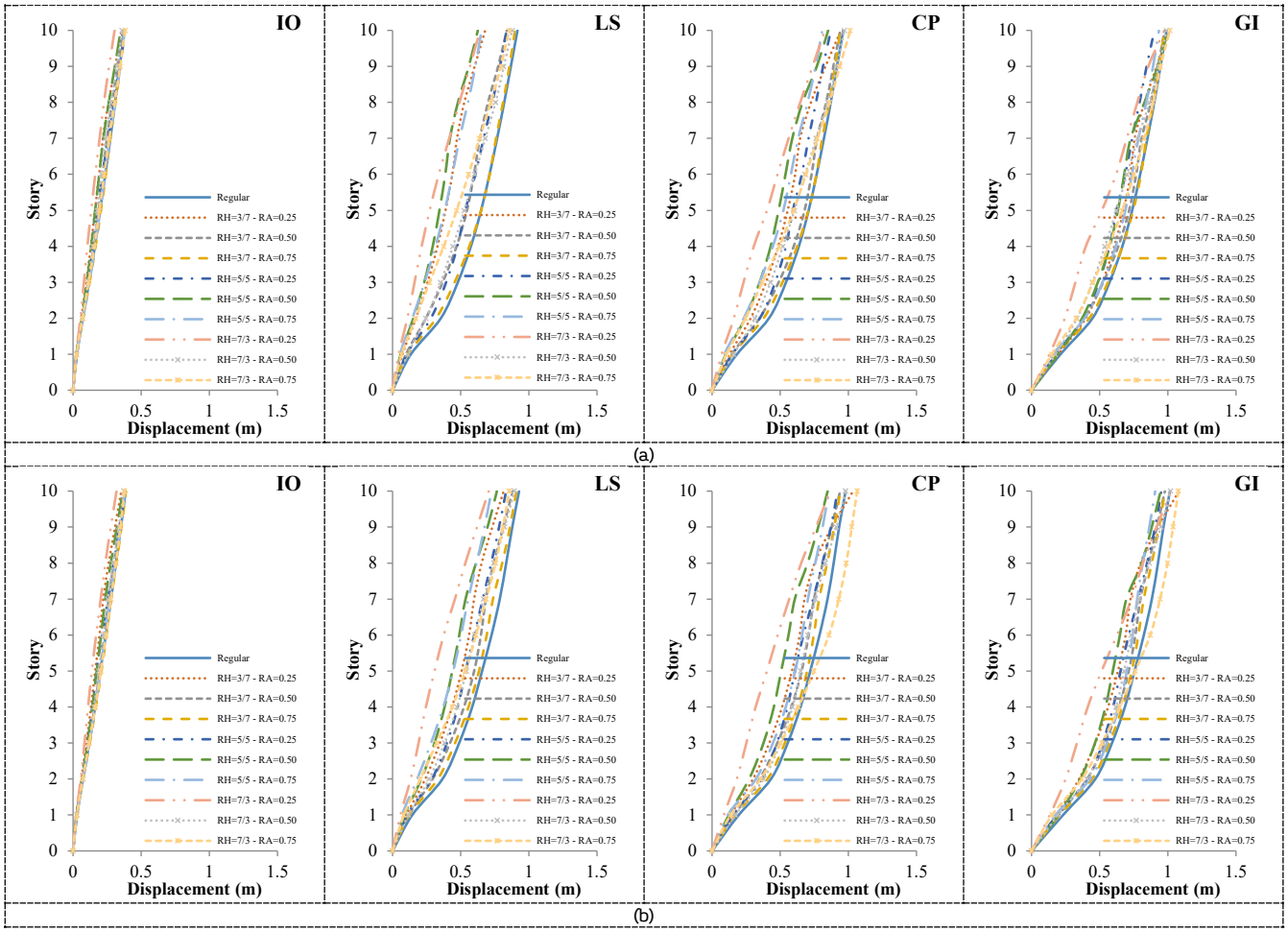

Figure 13. Comparison of the distribution of displacement demand over the structure height: (a) fixed-base buildings (b) flexible-base buildings

6.3. Maximum story shear and moment forces

In this section, the height-wise maximum shear and moment forces of flexible-base setback buildings are compared to those of the fixed-base at different performance levels. Figure 16 shows that SSI makes the story shear of the flexible-base setback buildings different from that of the fixed-base ones. A similar result is observed in the case of moment forces in Figure 17. The maximum base shear and moment forces of the flexible-base setback buildings reduce in comparison to those of the fixed base ones. The story shear and moment forces are more sensitive at the IO limit state. Due to the SSI effect, the force demand for setback buildings reduces up to 15%. The reduction rate is significant at the elastic and earlier inelastic phase of structural behavior in most setback buildings. However, the rate of force demand variation is not identical over the structure height. The difference between the fixed and flexible-base shear and moment forces is higher at the middle and lower story levels of setback buildings and reduces at the top floors. The study of the maximum force demands at the base level of structures shows that the more the RA index, the less the difference between the maximum base shear and moment forces of fixed and flexible base structures.

It is important to note that the reduction rate in the maximum shear and moment force reduces as the structures pass the LS limit-state. At this performance objective, the maximum shear force reduction rate is limited to 5%. A similar pattern is observed in the case of maximum moment force in setback buildings. However, the difference between the force demand for fixed and flexible-base structures reduces at the higher nonlinear phase of structure behavior. Thus, no considerable difference is observed between the fixed and flexible base setback buildings, at the CP to the GI limit-states.

The components of shear and moment force demands of regular and setback structures are shown correspondingly in Figure 18 and Figure 19 at each performance objective. In comparison with the regular structure, the force demands reduce in both cases of fixed and flexible-base setback buildings. A considerable portion of reduction is observed near the setback area. This is due to the mass reduction at the setback floors which reduces the effective seismic force at the story level. However, increasing the RA ratio or reducing the RH makes the force demand distribution pattern similar to that of the regular building.

It is worth mentioning that SSI shows to have a remarkable effect on the force demand for the regular building. It is observed that the force demands of flexible base regular building moderately reduces up to 8% in comparison with the fixed base model. Unlike the setback buildings, the force demand reduction rate is almost uniform over the structure height.

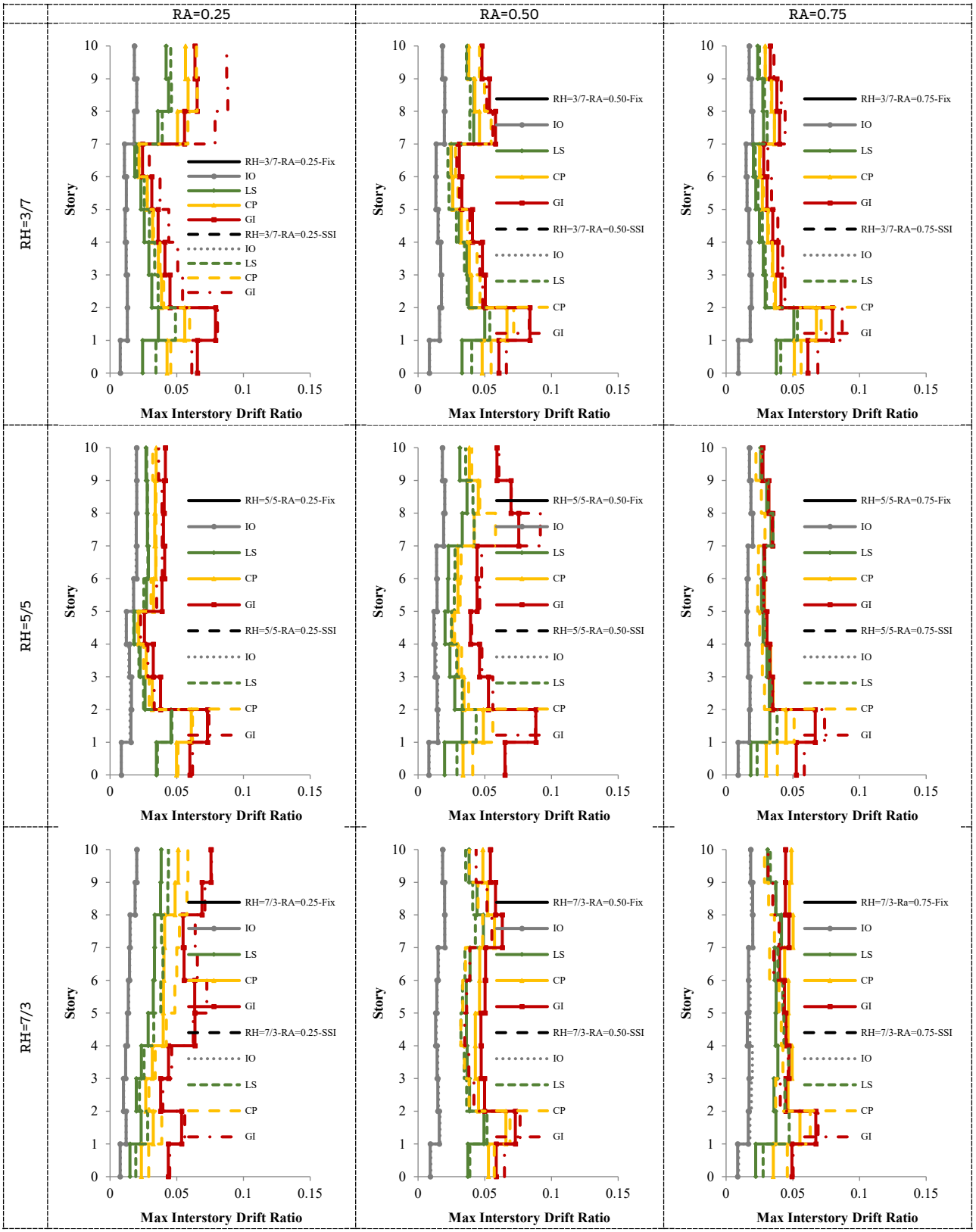

Figure 14. The distribution of drift demand over the height of fixed and flexible-base setback structures

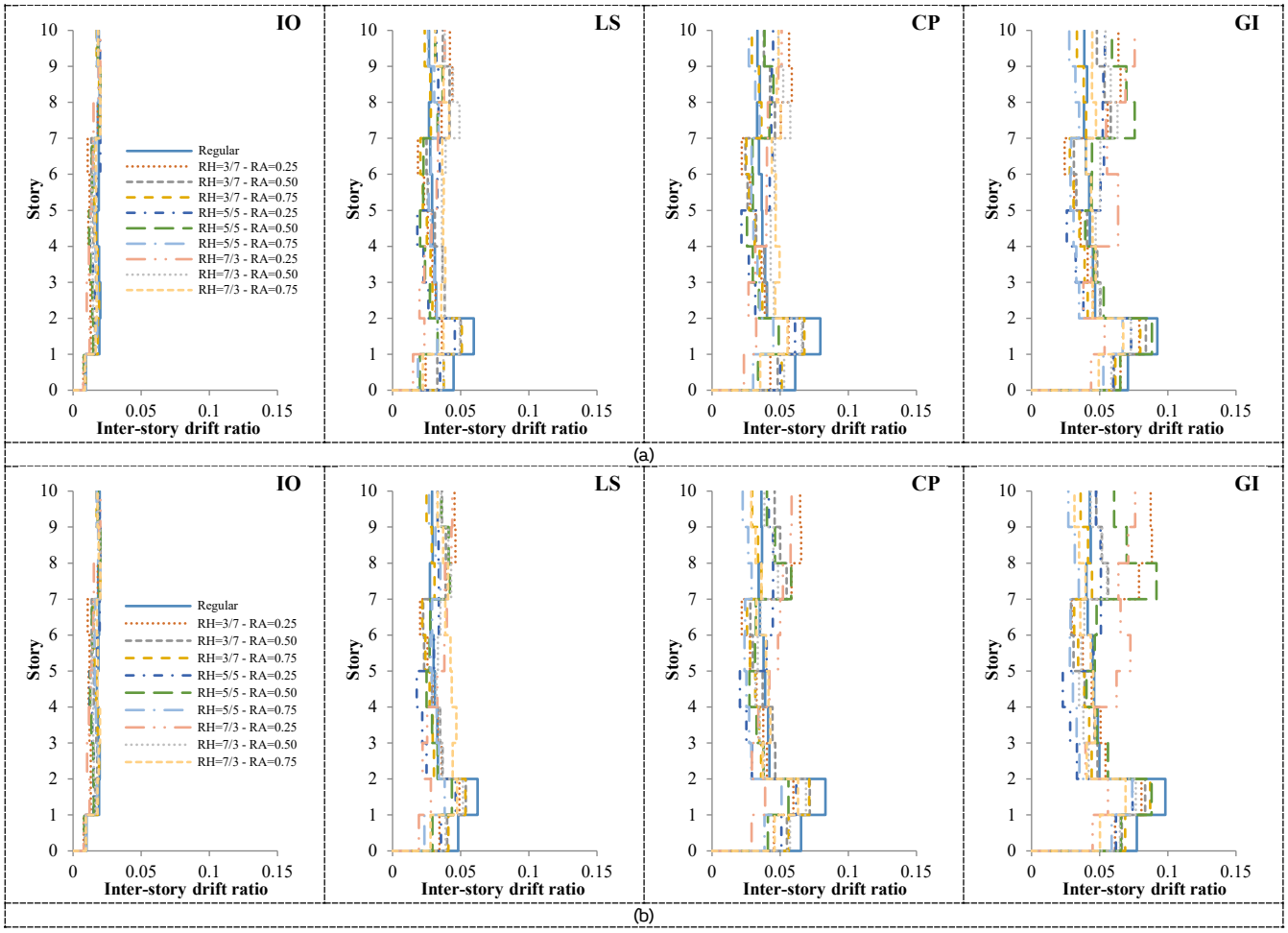

Figure 15. Comparison of the distribution of drift demand over the structure height: (a) fixed-base buildings (b) flexible-base buildings

6.4. Maximum plastic hinge rotation of beam and column elements

To assess the effect of SSI on the vulnerability of setback buildings, the maximum plastic hinge rotation of flexible-base buildings is compared to that of the fixed-base. Higher rotation of the element plastic hinges shows higher vulnerability concentration at the element. Figure 20 represents the distribution of maximum hinge rotation of the beam elements over the height of setback buildings. It is observed that SSI increases the beam plastic hinge rotation, especially at the LS to the CP performance levels. Although the maximum hinge rotation is observed at the bottom floor of setback buildings, a high portion of the damage is concentrated near the setback area and at the tower part of the structures. This shows higher vulnerability potential for the tower area especially in the case of structures with smaller RA.

SSI affects the maximum hinge rotation of beam elements as well. The maximum difference between the hinge rotation of fixed and flexible-base setback buildings is observed in the case of structures with higher RH, especially in the setback building with RH=7/3-RA=0.75. In this case, SSI increases the beam rotation from 30% at the linear phase to 60% at the nonlinear phase of behavior, in comparison with the fixed base structure. Meanwhile, the minimum effect of SSI is observed for regular building. In this case, the maximum increase rate in the beam hinge rotation is about 13%.

The maximum hinge rotation of regular and setback buildings is compared in Figure 21 for both cases of fixed and flexible base conditions. Although a similar result is observed for both the regular and setback buildings at the IO limit state, the distribution pattern and the degree of beam hinge rotation vary at the nonlinear phase of structural behavior. Unlike the regular structure, a large portion of rotation demand is concentrated at the top floors of setback buildings, especially at the setback floors.

Similar to the beam plastic hinge rotation case, the maximum hinge rotation of the column elements was presented in Figure 22. The plastic hinge rotation of column elements at a story shows the collapse potential of that floor under the applied lateral load. Results show that a large portion of demand is concentrated at the bottom floor of all the setback buildings with various base conditions. However, columns at the setback floors are vulnerable to seismic loads so that a considerable degree of rotation is observed at the tower part of setback structures. The setback structure with RH=5/5-RA=0.50 is remarkable in this case.

Similar to the beam elements, SSI increases the damage ratio of the column elements, as well. The minimum effect of SSI is observed at the IO limit state. In this case, the difference between the average column rotation of fixed and flexible base setback buildings is about 7%. However, the remarkable effect of SSI occurred in the setback structure with RH=7/3-RA=0.75 so that the column hinge rotation of the flexible base structure is 20% higher than the fixed base one. The level of increase in the column hinge rotation of the flexible base structure increases as the structure gets to the nonlinear phase of behavior.

About 115% and 100% increase was observed in the case of setback buildings with RH=5/5-RA=0.50 and RH=3/7-RA=0.25, correspondingly. This rate increases at the CP performance objective and about 145% difference is observed between the fixed and flexible base structures with RH=7/3-RA=0.75.

Nonetheless, the level of column hinge rotation decreases at the GI performance objective so that the maximum rate of 70% is observed in the case of setback building with RH=7/3-RA=0.50. The maximum hinge rotation of regular and setback buildings is compared in Figure 23 for both cases of fixed and flexible setback buildings. It is observed that damage is mostly concentrated on the bottom floor. Unlike the regular building, the distribution pattern and the degree of column hinge rotation increase at the top floors (tower area) of setback buildings, especially at the nonlinear phase of structural behavior.

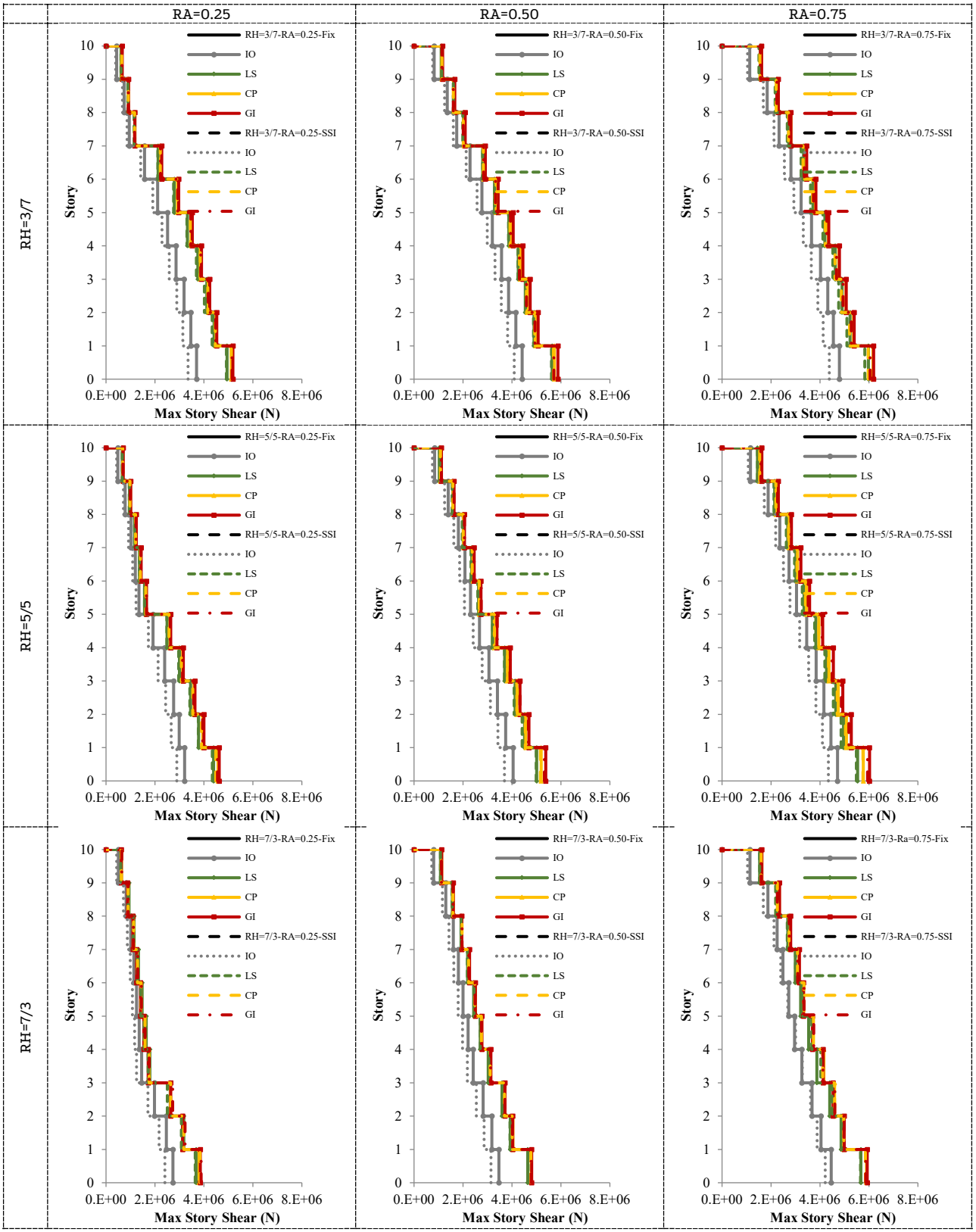

Figure 16. The distribution of shear force demand over the height of fixed and flexible-base setback structures

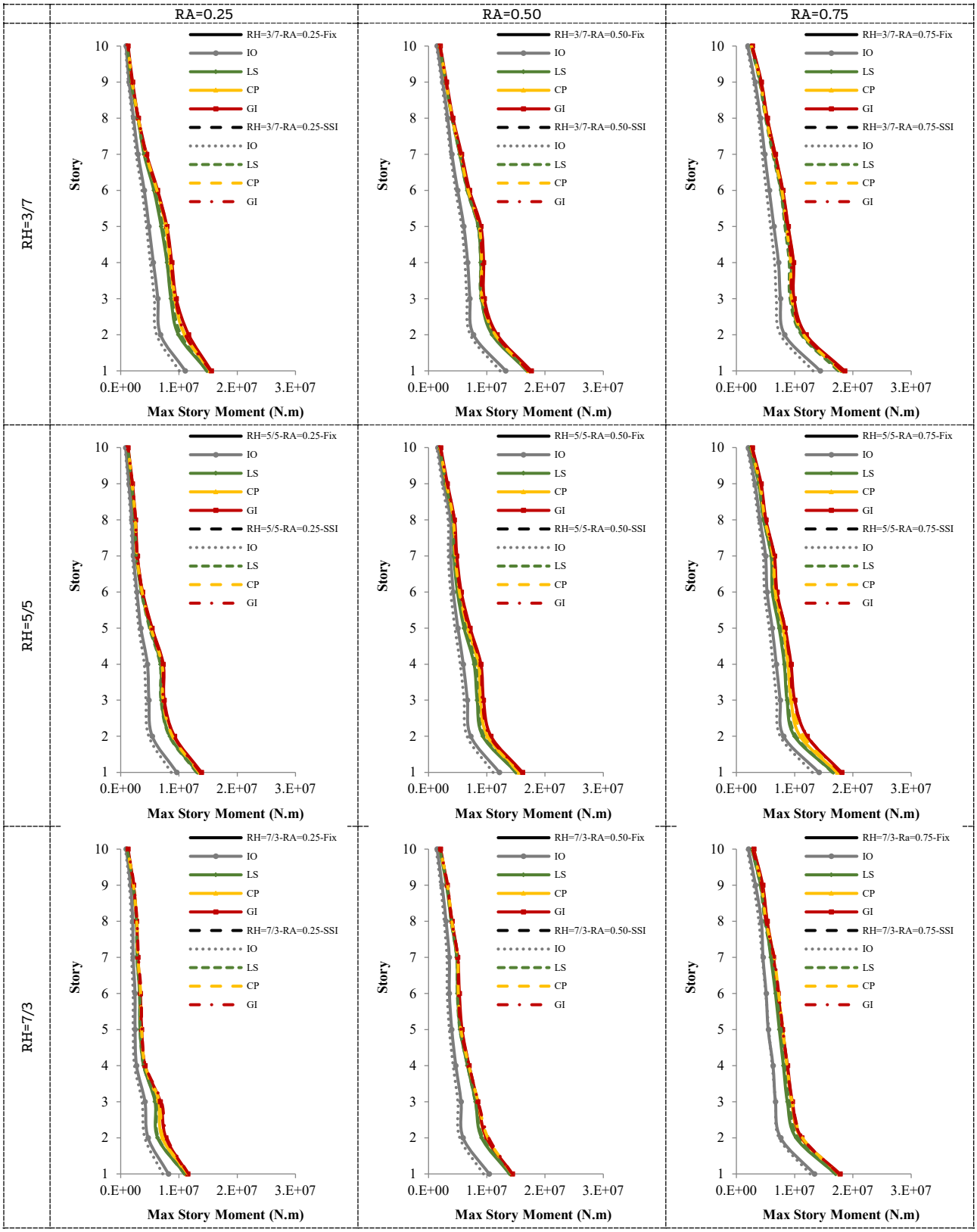

Figure 17. The distribution of moment demand over the height of fixed and flexible-base setback structures

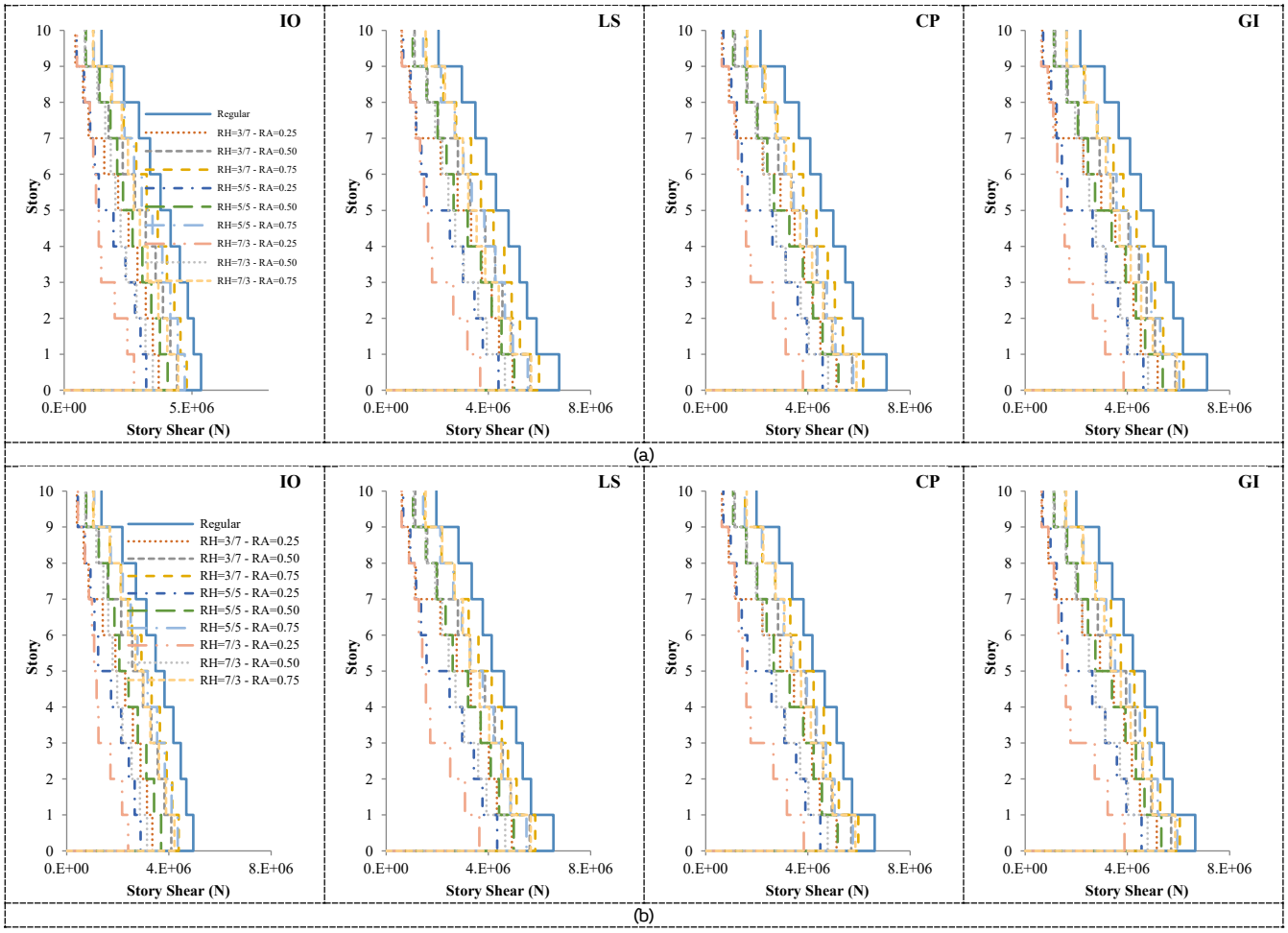

Figure 18. Comparison of the distribution of shear force demand over the structure height: (a) fixed-base buildings (b) flexible-base buildings

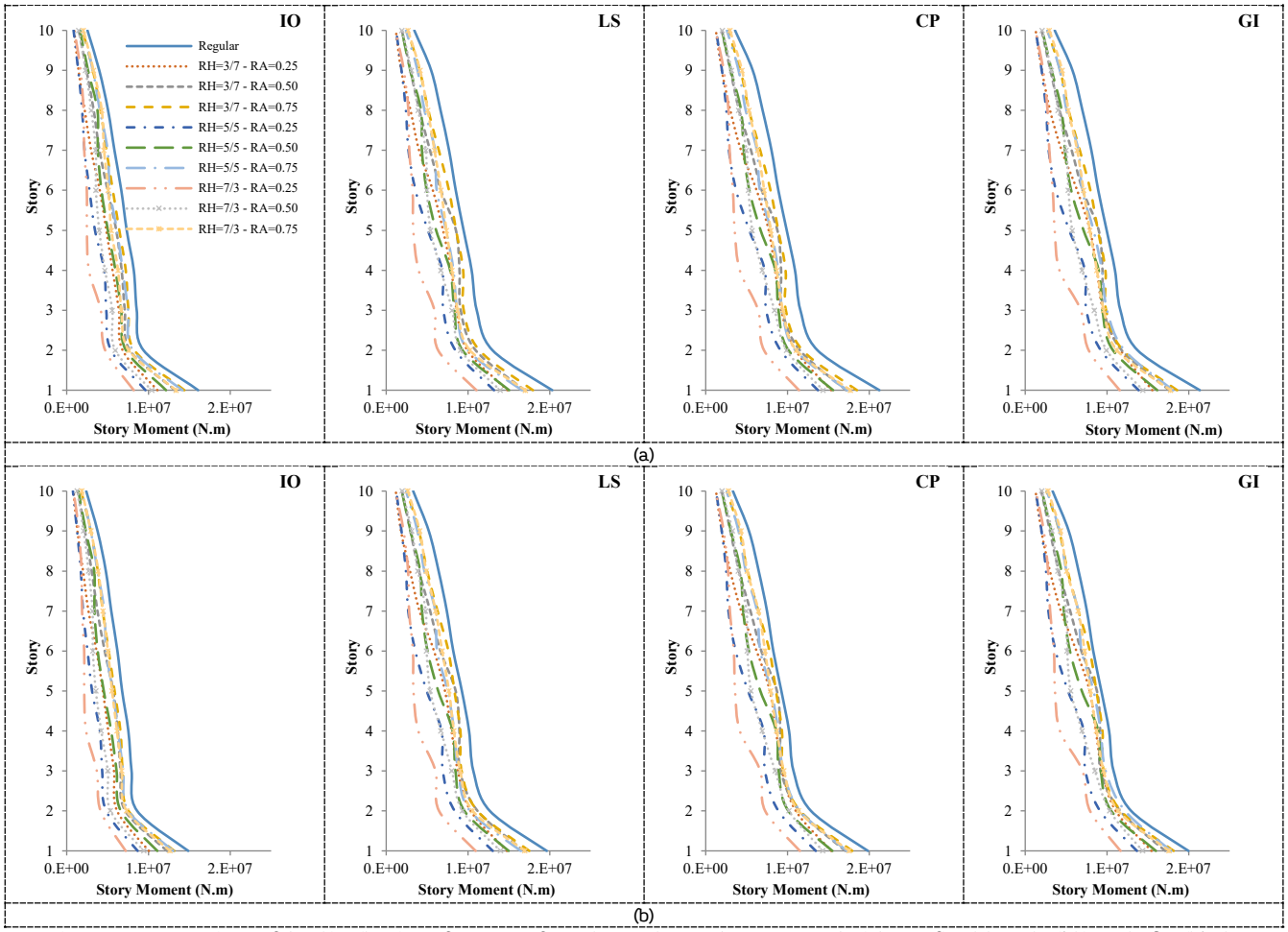

Figure 19. Comparison of the distribution of moment force demand over the structure height: (a) fixed-base buildings (b) flexible-base buildings

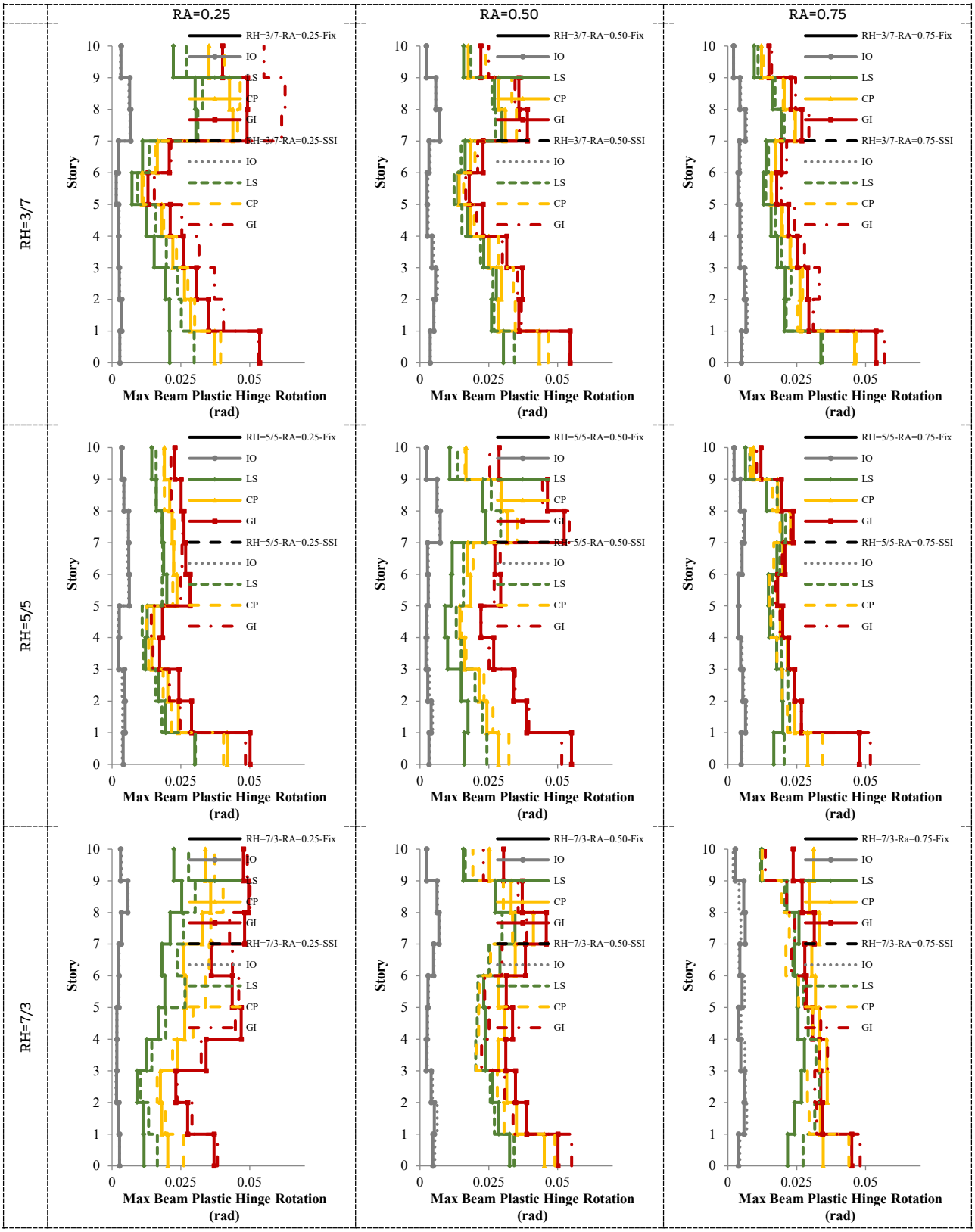

Figure 20. The distribution of maximum plastic hinge of beams over the height of fixed and flexible-base setback structures

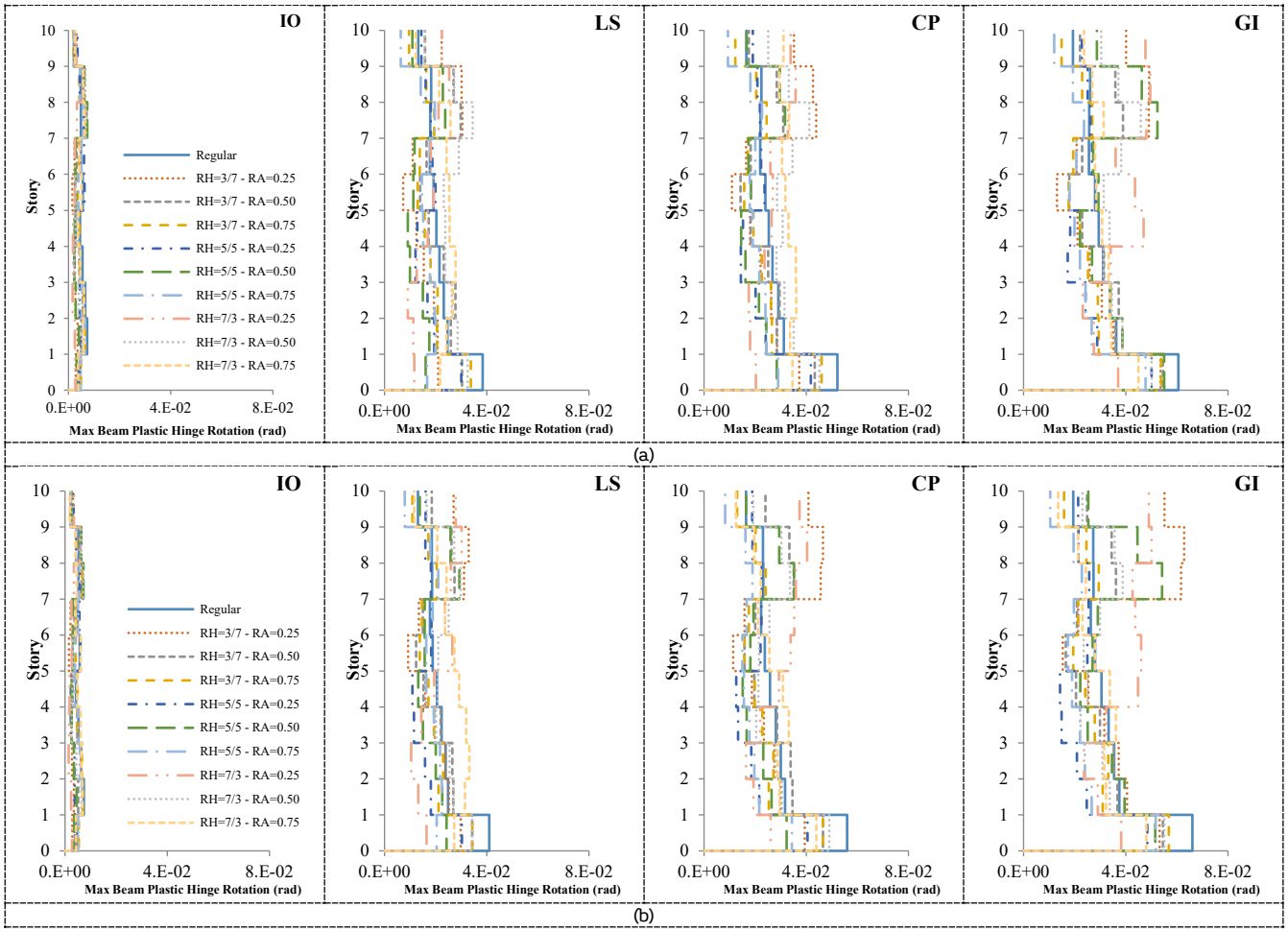

Figure 21. Comparison of the distribution of maximum plastic hinge rotation of beam elements over the structure height: (a) fixed-base buildings (b) flexible-base buildings

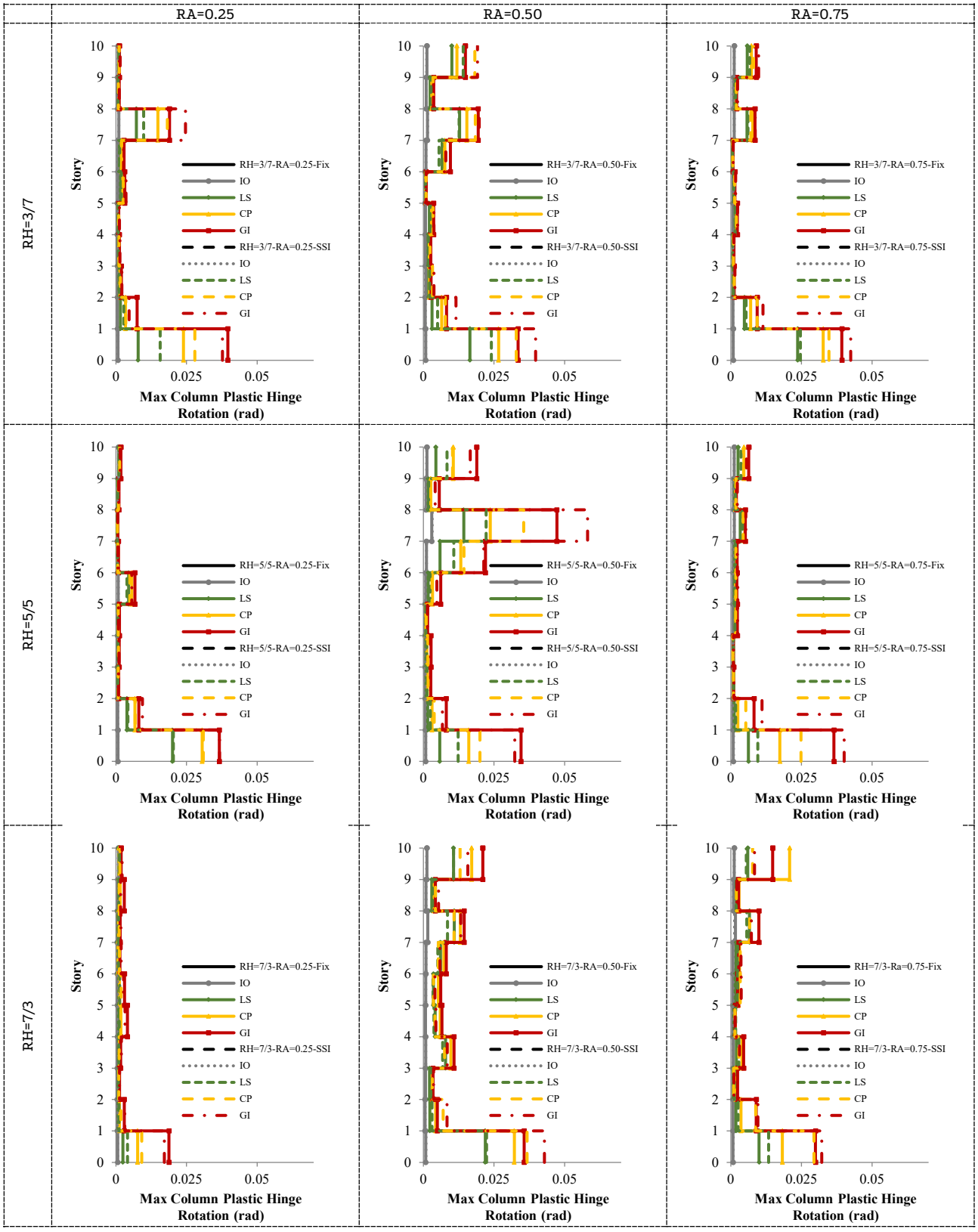

Figure 22. The distribution of maximum plastic hinge of columns over the height of fixed and flexible-base setback structures

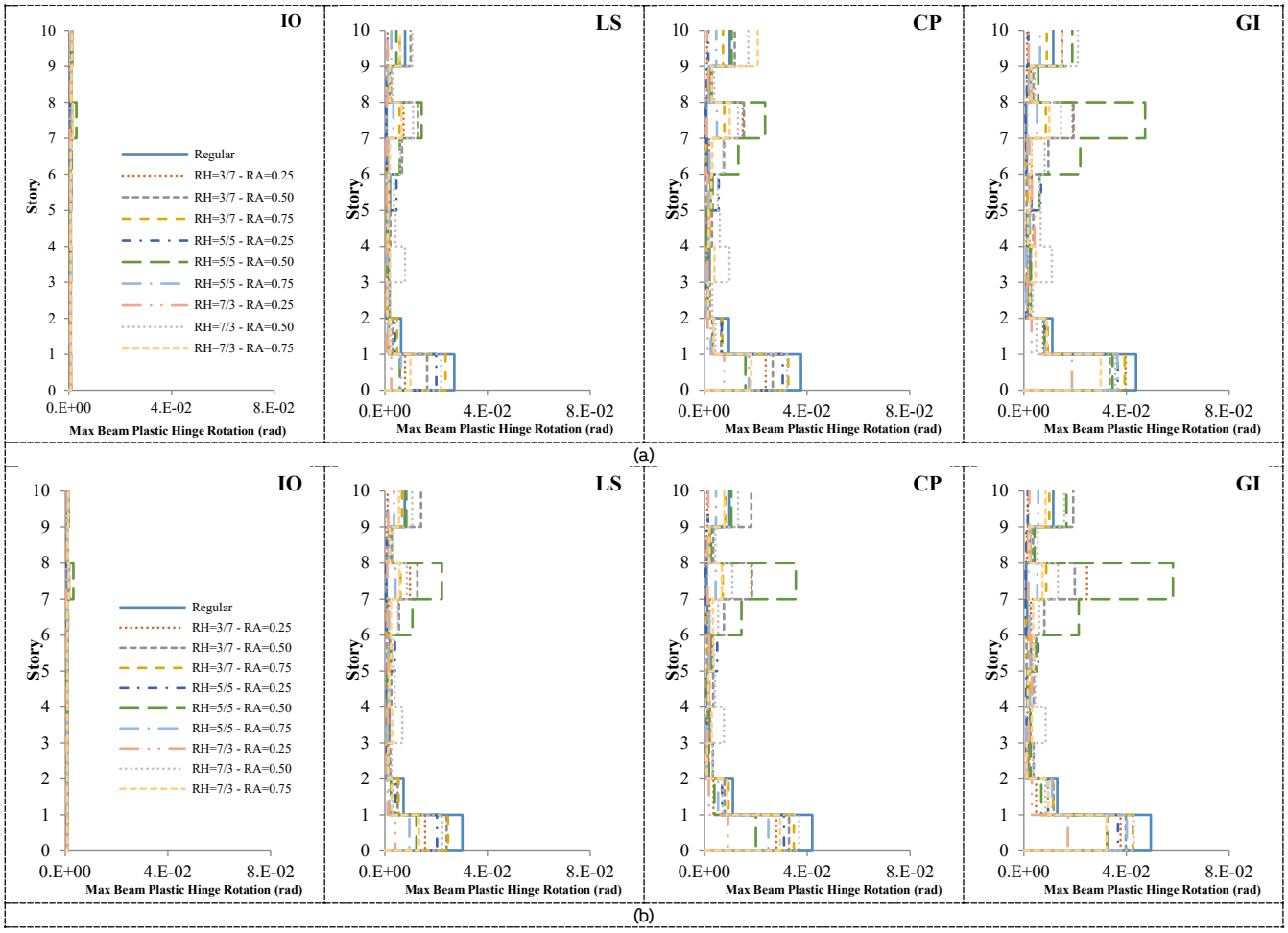

Figure 23. Comparison of the distribution of maximum plastic hinge rotation of column elements over the structure height: (a) fixed-base buildings (b) flexible-base buildings

7. Conclusion

In this study, the effect of SSI is evaluated on the height-wise seismic response of steel setback buildings. For this purpose, a group of setback buildings was analyzed nonlinearly under the horizontal components of earthquake ground motions. Foundation flexibility effects were considered by using the BNWF approach. Time history analysis of steel structures was carried out and the displacement and drift demand of flexible-base setback buildings were compared to those of the fixed-base ones at different performance levels. The maximum shear and moment forces were calculated at each story level to show the SSI effect on force demand distribution. Finally, the maximum plastic hinge rotation of beam and column elements was presented to show the SSI effect on the vulnerability level of structural elements and collapse mechanism in setback buildings at various performance objectives. Based on the given results, the following conclusions are drawn:

- Foundation flexibility alters the demand distribution pattern over the structure height. The level of nonlinear behavior of setback buildings plays a critical role in the rate of variation in the structural seismic response.
- The remarkable effect of SSI on the displacement demand is observed in structures with a higher RH. Thus, the design of top stories in flexible base buildings requires special attention since higher demand is observed after the LS limit-state.
- The maximum displacement of setback buildings is smaller than that of the regular structure. Therefore, it is concluded that considering a target displacement demand equal to that of the regular building can produce enough margin of safety for the code-based design setback building.
- SSI increases the drift demand for setback buildings from 15% in the elastic phase of behavior to 50% in the nonlinear region. Moreover, it changes the distribution pattern of drift demand over the structure height; depending on the nonlinear level of structure behavior; a point to be considered in the design procedure of setback buildings on soft soil.
- The concentration of drift demand at the bottom floor and near the setback area of setback structures shows a high level of damage at the adjacent floors. Therefore, the lateral force-resisting elements of these stories necessitate appropriate design in order to resist the applied force and deformations at the corresponding performance level.
- SSI reduces the shear and moment force demand in flexible-base setback buildings. The maximum rate of reduction is about 15% and observed at the elastic phase of structural behavior. However, the force demand reduction rate decreases at the nonlinear phase of structural behavior. Therefore, the margin of safety must be considered in reducing the force demand in the design of new structures.
- Due to the irregularity in setback buildings, the rotation of plastic hinges at the end of beam and column elements increases relative to the regular structure. Meanwhile, SSI modifies the maximum plastic hinge rotation of frame elements as well. The remarkable effect was observed at the LS to the CP performance levels, where 30% to 60% increase in the rotation of beam elements. A similar effect was observed in the case of column elements and the plastic hinge rotation increased up to 145%.

- Generally, SSI modifies the seismic response of setback buildings. Therefore, the design of these structures, especially on soft soils entails particular attention.

Declaration of Conflict of Interests

The author declares that there is no conflict of interest. They have no known competing financial interests or personal relationships that could have appeared to influence the work reported in this paper.

References

[1.] Karavasilis TL, Bazeos N, Beskos D. Seismic response of plane steel MRF with setbacks: estimation of inelastic deformation demands. Journal of Constructional Steel Research. 2008;64:644-54.

[2.] Humar J, Wright E. Earthquake response of steel-framed multistorey buildings with set-backs. Earthquake engineering & structural dynamics. 1977;5:15-39.

[3.] Shahrooz BM, Moehle JP. Seismic response and design of setback buildings. Journal of Structural Engineering. 1990;116:1423-39.

[4.] Shahrooz BM, Moehle JP. Experimental study of seismic response of RC setback buildings: Earthquake Engineering Research Center, College of Engineering, University of California; Springfield, Va.: available from the National Technical Information Service; 1987.

[5.] Duan X, Chandler A. Seismic torsional response and design procedures for a class of setback frame buildings. Earthquake engineering & structural dynamics. 1995;24:761-77.

[6.] Shakib H, Pirizadeh M. Probabilistic Seismic Performance Assessment of Setback Buildings under Bidirectional Excitation. Journal of Structural Engineering. 2013.

[7.] Dutta SC, Bhattacharya K, Roy R. Response of low-rise buildings under seismic ground excitation incorporating soil-structure interaction. Soil Dynamics and Earthquake Engineering. 2004;24:893-914.

[8.] Stewart JP, Fenves GL, Seed RB. Seismic soil-structure interaction in buildings. I: Analytical methods. Journal of Geotechnical and Geoenvironmental Engineering. 1999;125:26-37.

[9.] Homaei F, Shakib H. Evaluation of random seismic response of mid-rise buildings with mass irregularity considering soil-structure interaction effects. 2015.

[10.] Homaei F, Shakib H, Soltani M. Probabilistic Seismic Performance Evaluation of Vertically Irregular Steel Building Considering Soil–Structure Interaction. International Journal of Civil Engineering. 2017;15:611-25.

[11.] [12] Shakib H, Homaei F. Probabilistic seismic performance assessment of the soil-structure interaction effect on seismic response of mid-rise setback steel buildings. Bulletin of Earthquake Engineering. 2017;15:2827-51.

[12.] [13] Shakib H, Homaei F. Soil-structure interaction effects on demand and probabilistic confidence level of geometric vertically irregular steel buildings. Modares Civil Engineering journal. 2017;16:215-29.

[13.] [14] Mashhadi S, Asadi A, Homaei F, Tajammolian H. Seismic response of mid-rise steel MRFs: the role of geometrical irregularity, frequency components of near-fault records, and soil-structure interaction. Bulletin of Earthquake Engineering. 2021.

[14.] Homaei F. Estimation of the ductility and hysteretic energy demands for soil–structure systems. Bulletin of Earthquake Engineering. 2021.

[15.] Mashhadi S, Asadi A, Homaei F, Tajammolian H. The performance-based seismic response of special steel MRF: Effects of pulse-like ground motion and foundation safety factor. Structures. 2020;28:127-40.

[16.] Homaei F, Yazdani M. The probabilistic seismic assessment of aged concrete arch bridges: The role of soil-structure interaction. Structures. 2020;28:894-904.

[17.] Homaei F. Investigating the effects of inelastic soil–foundation interface response on the seismic demand of soil–structure systems. Canadian Journal of Civil Engineering. 2020:1-18.

[18.] Karapetrou ST, Fotopoulou SD, Pitilakis KD. Seismic vulnerability assessment of high-rise non-ductile RC buildings considering soil–structure interaction effects. Soil Dynamics and Earthquake Engineering. 2015;73:42-57.

[19.] Hokmabadi AS, Fatahi B, Samali B. Assessment of soil–pile–structure interaction influencing seismic response of mid-rise buildings sitting on floating pile foundations. Computers and Geotechnics. 2014;55:172-86.

[20.] Behnamfar F, Banizadeh M. Effects of soil–structure interaction on distribution of seismic vulnerability in RC structures. Soil Dynamics and Earthquake Engineering. 2016;80:73-86.

[21.] Nakhaei M, Ghannad MA. The effect of soil–structure interaction on damage index of buildings. Engineering Structures. 2008;30:1491-9.

[22.] FEMA-440. Improvement of nonlinear static seismic analysis procedures. Applied Technology Council (ATC-55 Project); 2005.

[23.] ATC-40. Seismic evaluation and retrofit of concrete buildings: Seismic Safety Commission, Applied Technology Council; 1996.

[24.] Code IoBN. Building National Code of Iran - Loads for Buildings. Institute of Building National Code; 2014.

[25.] BHRC. Standard 2800. 4th ed: Building and Housing Research Centre, Tehran, Iran; 2014.

[26.] ASCE7-10. Minimum Design Loads for Buildings and Other Structures. Reston, Virginia American Society of Civil Engineers; 2010.

[27.] Council BSS. The 2003 NEHRP recommended provisions for new buildings and other structures Part 1: Provisions (FEMA 450). 2003.

[28.] BHRC. Standard 2800. 3rd ed: Building and Housing Research Centre, Tehran, Iran; 2010.

[29.] Building National Code of Iran - Steel Design. Institute of Building National Code; 2014.

[30.] Committee A. Specification for Structural Steel Buildings (ANSI/AISC 360-10). American Institute of Steel Construction, Chicago-Illinois. 2010.

[31.] Jafari MK. Seismic microzonation of North of Tehran from the viewpoint of site conditions. IIEES, (in Farsi). 1999.

[32.] Jafari MK. Supplementary studies of Seismic microzonation of South of Tehran. IIEES, (in Farsi). 2002.

[33.] Torabi H, Rayhani MT. Three dimensional Finite Element modeling of seismic soil–structure interaction in soft soil. Computers and Geotechnics. 2014;60:9-19.

[34.] Building National Code of Iran - Foundation Design. Institute of Building National Code; 2014.

[35.] Mazzoni S, McKenna F, Scott MH, Fenves GL. Open System for Earthquake Engineering Simulation (OpenSees). Pacific Earthquake Engineering Research (PEER) Center: University of California, Berkeley, CA; 2000.

[36.] Chopra AK. Dynamics of structures: theory and applications to earthquake engineering. 2007. Prentice-Hall; 2007.

[37.] ASCE41-13. Seismic evaluation and retrofit of existing buildings. American Society of Engineers; 2013.

[38.] FEMA355C. State of the art report on systems performance of steel moment frames subject to earthquake ground shaking. Federal Emergency Management Agency Washington, DC, USA; 2000.

[39.] Lignos D, Krawinkler H, Whittaker A. Prediction and validation of sidesway collapse of two scale models of a 4-story steel moment frame. Earthquake Engineering & Structural Dynamics. 2011;40:807-25.

[40.] Lignos DG, Krawinkler, H. Sidesway collapse of deteriorating structural systems under seismic excitations. In: 172 RNT, editor. Stanford University, Stanford, CA.: The John A. Blume Earthquake Engineering Research Center; 2009.

[41.] Raychowdhury P, Ray-Chaudhuri S. Seismic response of nonstructural components supported by a 4-story SMRF: Effect of nonlinear soil–structure interaction. Structures. 2015;3:200-10.

[42.] Raychowdhury P. Seismic response of low-rise steel moment-resisting frame (SMRF) buildings incorporating nonlinear soil–structure interaction (SSI). Engineering Structures. 2011;33:958-67.

[43.] Gajan S, Raychowdhury P, Hutchinson TC, Kutter BL, Stewart JP. Application and validation of practical tools for nonlinear soil-foundation interaction analysis. Earthquake Spectra. 2010;26:111-29.

[44.] Raychowdhury P, Hutchinson TC. Performance evaluation of a nonlinear Winkler-based shallow foundation model using centrifuge test results. Earthquake Engineering and Structural Dynamics. 2009;38:679-98.

[45.] Raychowdhury P. Effect of soil parameter uncertainty on seismic demand of low-rise steel buildings on dense silty sand. Soil Dynamics and Earthquake Engineering. 2009;29:1367-78.

[46.] [CW H, T H, GR M, BL K. Numerical modeling of the nonlinear cyclic response of shallow foundations. Technical Report 2005/04, Pacific Earthquake Engineering Research Center (PEER)2005.

[47.] Boulanger RW, Curras CJ, Kutter BL, Wilson DW, Abghari A. Seismic soil-pile-structure interaction experiments and analyses. Journal of Geotechnical and Geoenvironmental Engineering. 1999;125:750-9.

[48.] Boulanger R. The PySimple1, TzSimple1, and QzSimple1 material models, documentation for the OpenSees platform. URL: http:// opensees berkeley edu. 2000.

[49.] Mazzoni S, McKenna F, Scott MH, Fenves GL. OpenSees command language manual. Pacific Earthquake Engineering Research (PEER) Center. 2006.

[50.] Terzaghi K. 1943, Theoretical Soil Mechanics, John Wiley & Sons, New York.

[51.] PEER Ground Motion Database. Pacific Earthquake Engineering Research Center - http://ngawest2.berkeley.edu/.

[52.] Venture NCJ. Selecting and scaling earthquake ground motions for performing response-history analyses. NIST GCR. 2011:11-917.

[53.] Rezaeian S, Der Kiureghian A. Simulation of synthetic ground motions for specified earthquake and site characteristics. Earthquake Engineering & Structural Dynamics. 2010;39:1155-80.

[54.] Lignos DG, Krawinkler H. Deterioration modeling of steel components in support of collapse prediction of steel moment frames under earthquake loading. Journal of Structural Engineering. 2010;137:1291-302.

[55.] FEMA350. Recommended seismic design criteria for new steel moment-frame buildings: Federal Emergency Management Agency Washington, DC, USA; 2000.

[56.] FEMA351. Recommended seismic evaluation and upgrade criteria for existing welded steel moment-frame buildings. FEMA-351. 2000.

[57.] Vamvatsikos D, Cornell CA. Incremental dynamic analysis. Earthquake Engineering & Structural Dynamics. 2002;31:491-514.